

RF FIELD MEASUREMENT AND ITS ANALYSIS ON
A MODEL RESONATOR OF THE INTERDIGITAL H TYPE LINAC

N. Ueda, S. Yamada, E. Tojyo, T. Hattori, K. Yoshida
Institute for Nuclear Study, University of Tokyo
Tanashi, Tokyo 188, Japan
and
T. Hori
Sumitomo Heavy Industries, Ltd.
1, Kanda Mitoshiro-cho, Chiyoda-ku, Tokyo 101, Japan

Summary

RF field measurement and its analysis have been made on a model resonator of the interdigital H (IH) type linac in order to study the feasibility of the IH type as the injector linac for the NUMATRON. The measurement shows that the inductance of the resonator is dominated by the cross sectional area. It also shows that the capacitance is concentrated near the drift tubes and agrees with the one measured electrostatically. The resonant frequencies are well explained with an equivalent circuit analysis based upon the field distribution measurement. Electrostatic capacitance has been measured on the models of the drift tubes with quadrupole magnets for the velocity range of $\beta = 2-16\%$. The effective shunt impedance has been calculated by using the electrostatically measured capacitance. The result is $150-70 \text{ M } \Omega/\text{m}$ for $\beta = 2-6\%$, which is two times higher than that of Wideröe type, $65-40 \text{ M } \Omega/\text{m}$ for $\beta = 6-10\%$, which is 1.5 times higher than that of Alvarez type.

Introduction

The NUMATRON is a high energy heavy ion accelerator proposed at INS.¹ It consists of an injector linac and two synchrotrons which accelerate heavy ions including uranium up to 1-2 GeV per nucleon. The injector linac is required to accelerate heavy ions from several keV up to 10 MeV per nucleon. A design which employs Wideröe and Alvarez types has been given for the injector.

The IH type linac, namely linac using H (TE) mode RF field is suitable for low energy heavy ion accelerator because of its small transversal dimension for a given frequency and high shunt impedance.² It has been demonstrated that an IH type linac has much higher shunt impedance than alvarez type in the velocity region of $\beta = 5-10\%$.³ In order to study the feasibility of the IH type as an injector linac for the NUMATRON, RF field measurement and its analysis were made on a 1/8 scaled model resonator.

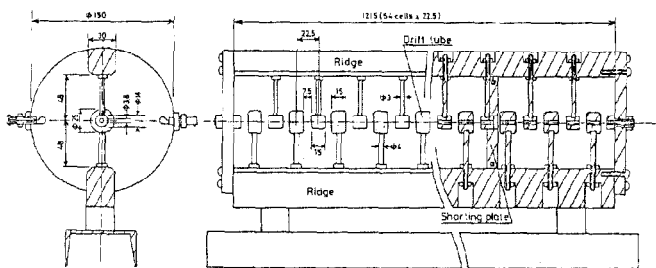


Fig. 1 Schematic view of the model resonator.

Model Resonator

The resonator length is variable from 180 mm to 1215 mm by moving a shorting plate. The inner diameter is 150 mm and the cross sectional area is also variable by using shorting plates. Drift tubes of 25 mm dia. and 14 mm dia. are aligned alternately in $\pi-\pi$ mode with a constant cell length of 22.5 mm. The bigger one corresponds to the diameter of 200 mm in full scale which can contain a quadrupole magnet. The cell length corresponds to $\beta = 3\%$ for an operating frequency of 25 MHz. The gap to cell length ratio is 1/3. The resonator is made of brass (Fig. 1).

Resonant Frequency

The resonant frequencies were measured for various resonator lengths, cross sectional areas and ridge dimensions. The Q value is 1800 for the maximum length and cross section. In Fig. 2 the resonant frequencies of TE_{11n} mode are plotted versus n/ℓ , where ℓ is the resonator length. It is shown that the resonant frequencies for various lengths depend on n/ℓ with a fixed ridge dimension and cross sectional area. They are fitted well by a following relation.

$$f = f_0 \left[\frac{1 + a(n/\ell)^2}{1 + b(n/\ell)^2} \right]^{1/2}$$

By the least square method f_0 , a and b were determined. In Fig. 3 it is shown that the cut off frequency f_0 is inversely proportional to the square root of the half cross sectional area.

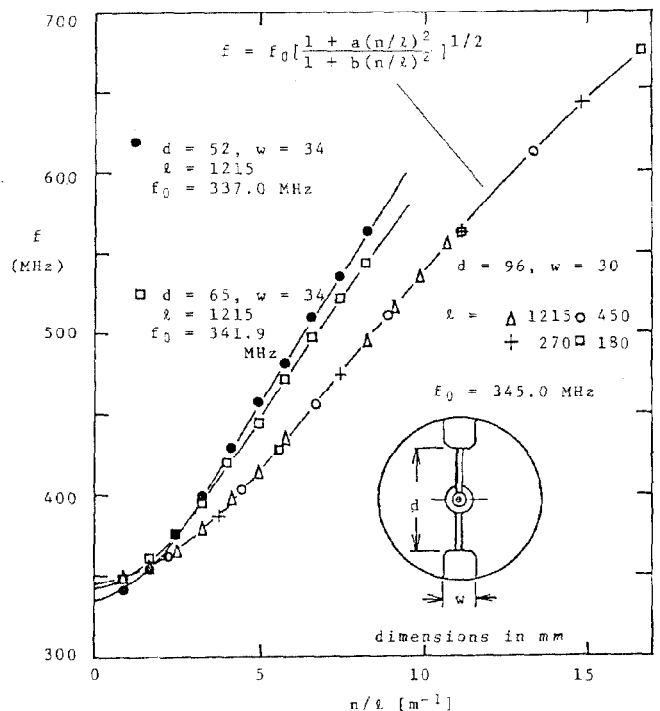


Fig. 2 Resonant frequencies for various resonator lengths and ridge dimensions.

Field Distribution

The magnetic field distribution was measured by the perturbing ball method with a small ferrite cylinder as a perturber. The magnetic field strength is homogeneous on a cross section and sinusoidal along the axis (Fig. 4). The resonant frequency shifts were measured with a teflon tube stretched over the length. The shift is proportional to the integrated electric field energy over the length on a point of the cross section. The electric field energy is sharply concentrated near the drift tubes (Fig. 5).

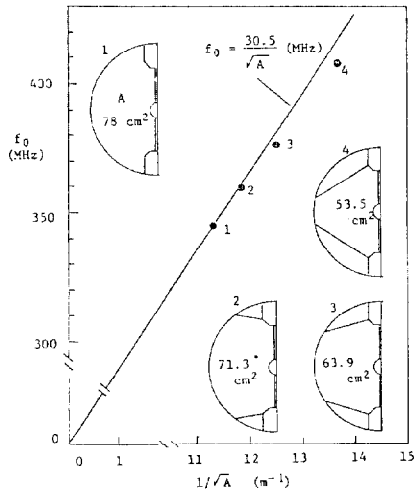


Fig. 3 Cut off frequency f_0 vs. the half cross sectional area A .

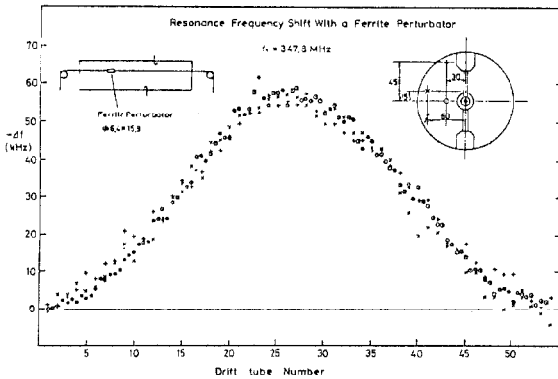


Fig. 4 Magnetic field distribution measured by the perturbing ball method.

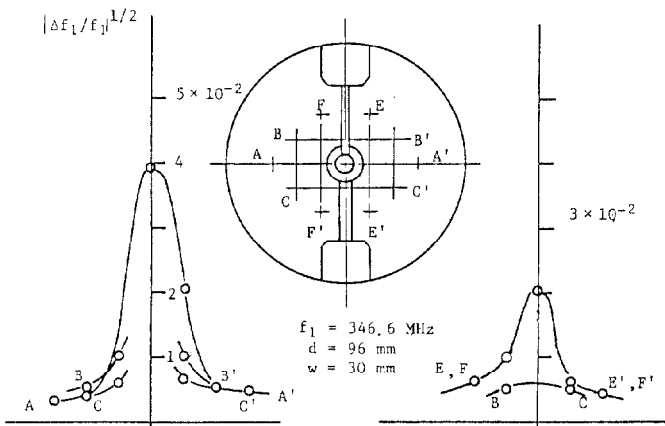


Fig. 5 Electric field distribution on the cross section.

Equivalent Circuit Analysis

On the basis of the field distribution measurement an equivalent circuit was adopted (Fig. 6). The voltage across the drift tube gap V_g is determined by a following differential equation derived from the equivalent circuit with an infinitesimal cell length.

$$\frac{d^2 V_g}{dz^2} + K^2 V_g = 0$$

where z is the coordinate along the axis. The phase advance per unit length K is given as follows.

$$K^2 = \frac{\omega^2 - \omega_0^2}{1 - 4\omega^2 L_S C_d} \cdot L_R C_d, \quad \omega_0^2 = \frac{1}{(L_p + 8L_S) \cdot C_d / 2}$$

when the geometry is constant along the length, the resonant frequency in the case of shorted ends is given as follows.

$$f = f_0 \left[\frac{1 + ((L_p + 8L_S)/2L_R) (n\pi/l)^2}{1 + (4L_S/L_R) \cdot (n\pi/l)^2} \right]^{1/2}$$

$$f_0 = \omega_0 / 2\pi$$

The dependence of the resonant frequency on n/l agrees with the experimental one. By comparing the dependence of f_0 on the inductance $L_p + 8L_S$ with the experimental result, we assume

$$L_p + 8L_S = \mu_0 A$$

Then the capacitance C_d is obtained from f_0 . These calculated capacitances agree well with electrostatically measured ones for various ridge dimensions (Fig. 7). The electrostatic measurement was done with the ridges supported by insulators and the outer conductor removed.

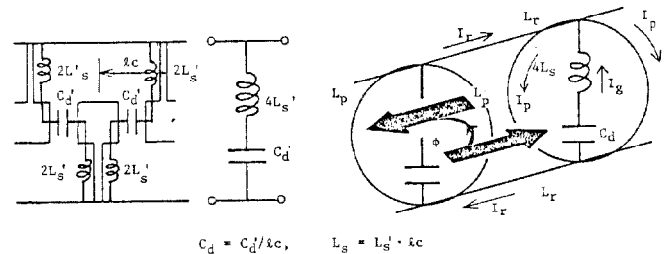


Fig. 6 Equivalent circuit for the IH structure. The values I_p , I_g , L_p , L_S and C_d are given for unit length.

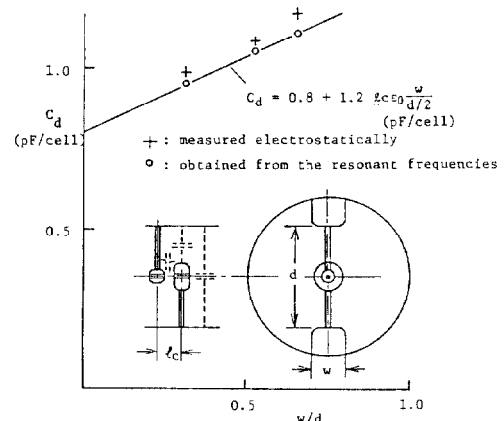


Fig. 7 Capacitances obtained from the resonant frequencies and measured electrostatically.

Electrostatic Capacitance Measurement

The capacitance C_d is composed by the gap capacitance between adjacent drift tubes, the capacitance between the ridges and drift tubes and the capacitance between the ridges. In order to estimate the effective shunt impedance in the range of $\beta = 2 - 16\%$, the capacitances were measured electrostatically on 1/8 scaled drift tube models. The cell length of the models are 15, 30, 45 and 60 mm, which correspond to $\beta = 2, 4, 6$ and 8% for the operating frequency of 25 MHz, and 4, 8, 12 and 16% for 50 MHz. The diameter of the drift tubes, the dimensions of the ridges and stems are variable. The gap to cell length ratio is 1/3. The measurement was done with ten cells for each cell length. The results are shown in Fig. 8. The capacitance per cell for the full scale drift tube is 8 times of that for the model and the capacitance per unit length is the same as that for the model.

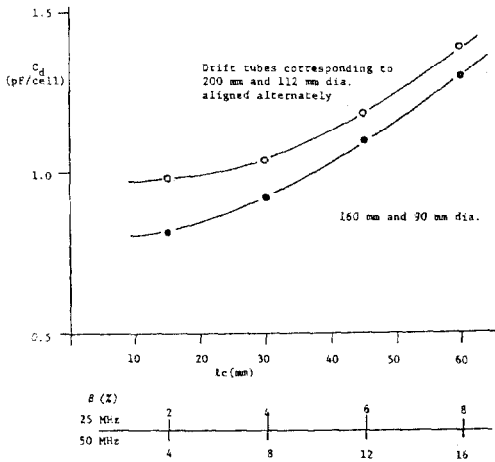


Fig. 8 Capacitances around the drift tubes measured electrostatically.

Shunt Impedance

The shunt impedance of the IH type is given as follows.

$$Z = \frac{4}{\pi(\pi+2)\sqrt{\rho}} \frac{1}{(\beta c)^2} \frac{f^{1/2}}{C_d^{3/2}} \frac{1}{k_d k_s k_c k_r}$$

where f is the operating frequency, βc is the particle velocity, ρ is the electric resistivity of the surface material, C_d is the capacitance around the drift tubes, k_s, k_c, k_r are the correction factors for the power loss increases due to the larger current density on the stems, the imperfect contact and surface roughness, the current along the ridges respectively, and

$$k_d = \left(\int_0^l I_p^2 dz / l \right) / \left(\int_0^l I_p^2 dz / l \right)^2$$

The expression turns out to be the same as that given by E. Nolte et al., by using the relations, the resonator diameter $D = 2/(\pi f \sqrt{\pi k_d})$ and the half cross section $A = \pi D^2/8$. The shunt impedance for $\pi - 3\pi$ mode is one fourth of the value given above. The effective shunt impedance is defined as

$$Z_{eff} = T^2 Z$$

where T is the transit time factor.

The effective shunt impedance was calculated on the basis of the electrostatic capacitance measurement (Fig. 9). The calculation was done by assuming that the field distribution is sinusoidal, namely,

$$k_d = \pi^2/8$$

$k_s \cdot k_c \cdot k_r = 2$ and $T = 0.9$. An operating frequency of 25 MHz was chosen for $\beta = 2 - 6\%$ and 50 MHz for $\beta = 6 - 16\%$. Drift tube diameters were chosen as 200 mm and 160 mm for the lower and the higher velocity region respectively, which can contain quadrupole magnets required by the beam dynamics.

Conclusion

The calculated effective shunt impedance of the IH type linac are 150 - 70 M Ω /m for $\beta = 2 - 6\%$, which is two times higher than that of Wideröe type the competitor in this region. For $\beta = 6 - 10\%$ the IH type has 1.5 times higher shunt impedance than Alvarez type. The IH type linac should be a most feasible candidate as the injector linac for the NUMATRON owing to its higher shunt impedance and simple structure of relatively small dimension.

Acknowledgement

The authors would like to thank Professors Y. Hirao, A. Mizobuchi and T. Katayama for useful discussions. They are much indebted to the skilled members of the machine shop at INS.

References

1. Y. Hirao et al., INS Report, NUMATRON. INS-NUMA-5 (1977)
2. M. Bres et al., Particle Accelerators, 2 (1971) 17-29.
3. E. Nolte et al., Nuclear Instrum. and Methods, 158 (1979) 311-324.

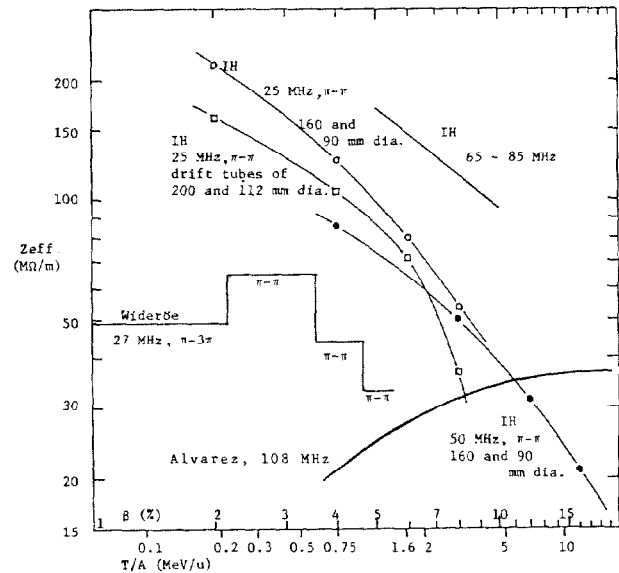


Fig. 9 Effective shunt impedance of the IH type linac.